excited-state spectra and excited-state splittings observed for five versus six coordination provide information on the coordination number of the ferrous complex. Differences in the spectra observed for FeSD and SBL indicate distinct structures for these ferrous active sites, FeSD being five coordinate square pyramidal and SBL being distorted octahedral. These spectra also contain detailed geometric structural information relating to effective symmetry at the ferrous site, which defines a limiting electronic symmetry of ligand field interactions. This may be distinct from the geometric information obtained from crystallographic studies, but it relates more directly to the chemistry of the metal center in its electronic structural origins. These comments are especially pertinent to the data for FeSD, for which crystallographic structures are emerging,[7-9] The electron density map for ferric SD at 3 Å resolution has been interpreted in terms of five coordination at iron, and no significant change is detected at this resolution in a difference density map for the ferrous derivative.[9] The results of our MCD studies, which require five coordination for the ferrous site, are consistent with the crystallographic data, indicating that the coordination number of the iron does not change on reduction. This contrasts with the decrease in coordination number observed for the active site of Cu-Zn SD on reduction,[53] relating to loss of a histidine imidazole ligand. Refinement of the crystal structure for ferric SD has led to a prediction of trigonal-bipyramidal geometry for the iron;[9] however, the actual site symmetry is expected to be lower and in fact the MCD spectroscopic data are consistent with an effective symmetry for the iron which is closer to a square-pyramidal electronic symmetry with $d_{xz,yz}$ containing the extra electron involved in electron transfer to O_2^-.

The sensitivity of the ligand field excited state spectra and the ground state properties on the environment of the iron makes temperature-dependent MCD particularly powerful as a probe of changes in structure associated with ligand binding. the apparent absence of ligand binding in the ferrous derivatives of FeSD and SBL has important mechanistic implications, suggesting that the redox reactivity of these sites involves outer-sphere electron transfer rather than an inner-sphere mechanism. Kinetic analysis by Fee et al. of superoxide dismutation by FeSD has already suggested that anions do not bind to the ferrous site;[11,17,18] the direct probe of ligand binding afforded by the spectroscopic approaches reported here is consistent with an outer-sphere mechanism for FeSD in its reducing cycle. This outer-sphere redox chemistry, while different from the proposed mechanism for Cu-Zn SD, would be consistent with protecting the site from Fenton-type chemistry[54,55] by peroxide reaction with Fe^{2+} as well as inhibition by the peroxide-Fe^{3+} product complex.

A comparison of the results for FeSD and SBL emphasizes that, while both suggest outer-sphere reactivity, a key distinction must be made between the ferrous derivatives of the two resting enzymes. Both of these active sites appear to interact with dioxygen species in the ferrous oxidation state. However, ferrous SBL is stable toward the reaction with O_2 leading to autoxidation; this difference in O_2 reactivity appears to relate to the increased coordination number for this ferrous site relative to SD, apparently relating to an increase in the number of imidazole ligands stabilizing Fe^{2+}. Further, for SBL the active ferrous species is associated with bound substrate radical which appears to be formed during turnover by substrate oxidation. Thus, the anaerobic substrate active site complex, rather than the resting enzyme, is thus the species most closely related to the structure of the ferrous site involved in the enzyme mechanism. Parallel absorption, CD, and variable-temperature, variable-field MCD experiments probing substrate and analogue interactions with ferrous sites in several mononuclear non-heme iron enzymes are in progress.

Acknowledgment. This work is supported by the National Institutes of Health (Grant GM40392). J.W.W. thanks the NIH for a postdoctoral fellowship (Grant AMO7456).

Guyanin, a Novel Tetranortriterpenoid: Structural Characterization by 2D NMR Spectroscopy and X-ray Crystallography

Stewart McLean,*,† Marion Perpick-Dumont,† William F. Reynolds,*,† Jeffery F. Sawyer,† Helen Jacobs,‡ and Frank Ramdayal‡

Contribution from the Department of Chemistry, University of Toronto, Toronto, Ontario, Canada M5S 1A1, and Centre for Natural Products Chemistry, University of Guyana, Georgetown, Guyana. *Received September 14, 1987*

Abstract: The skeletal structure of guyanin, a tetranortriterpene of an unprecedented structural type, has been unambiguously deduced by using ^{13}C-^1H shift-correlated spectra with delay times optimized for polarization transfer via two-bond and three-bond ^{13}C-^1H coupling. Spectra were obtained by using a modified version of our XCORFE pulse sequence. X-ray crystallography was used to confirm the structure and establish the stereochemistry of guyanin. The conformation in solution is the same as in the solid state, with ^1H-^1H coupling constants, NOE data, and ^{13}C T_1 relaxation times all suggesting that the molecule has little conformational mobility. Possible biogenetic origins of this unique molecule are discussed.

There has been intense interest in the application of two-dimensional (2D) NMR techniques to the elucidation of structures of complex organic molecules.[1] These techniques correlate a variety of combinations of ^1H and ^{13}C spectral properties by the application of specialized pulse sequences. The scope, value, and limitations of each technique in structural elucidation depend upon the type of data correlated, the dependability of the correlations (i.e., the degree of suppression of spurious correlations), and the sensitivity of the experiment. In most cases, the utility of a particular new technique has been illustrated by a detailed

† University of Toronto.
‡ University of Guyana.

(1) Morris, G. A. *Magn. Reson. Chem.* **1986**, *24*, 371.

0002-7863/88/1510-5339$01.50/0

spectroscopic analysis of a complex molecule of known structure.

We have recently developed a pulse sequence, XCORFE, which is designed to optimize the sensitivity and information content of ^1H–^{13}C chemical shift-correlated 2D spectra between hydrogen and carbon nuclei separated by two or three bonds.[2] This technique provides information that is clearly of immense value for structure elucidation since it identifies for a specific carbon atom those protonated carbon atoms which are either directly bonded to it or separated from it by two bonds. Its power is illustrated here by its application to the elucidation of the skeletal structure, entirely by NMR spectroscopy, of guyanin, **1**, a tet-

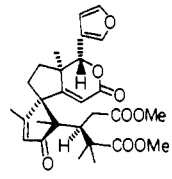

1

ranortriterpene of an unprecedented structural type.[3] The molecular conformations of **1** in solution and in the solid state are also compared, and the possible biosynthetic origins of this highly unusual molecule are discussed.

Results and Discussion

(a) Preliminary Characterization of 1. Guyanin was isolated from the roots of *Hortia regia* Sandwith (Rutaceae). Low resolution mass spectrometry indicated a molecular weight of 498. A combination of normal and DEPT-edited[4] ^{13}C spectra showed the presence of seven CH_3 groups, three CH_2 groups, seven CH groups, and 11 nonprotonated carbons, i.e., $C_{28}H_{34}$, corresponding to 370 amu. The remaining mass (128 amu) was assumed to be due to eight oxygen atoms, yielding a tentative empirical formula of $C_{28}H_{34}O_8$.

Further initial characterization involved recording of a ^1H spectrum plus a ^1H–^{13}C shift-correlated spectrum[5] which established connectivities between directly bonded carbons and hydrogens. Results of the various experiments are summarized in Table I. A number of structural features are readily apparent from these ^1H and ^{13}C spectral data. There are obviously four methyl groups bonded to quaternary carbons, while one methyl group (^1H doublet at δ 2.04 with J = 1.3 Hz) is at an olefinic site. This is coupled to a vinylic proton at δ 5.87. A second vinylic proton is seen as a singlet (δ 5.90), and a set of weakly coupled protons (δ 6.38, 7.44, 7.56) are consonant with the presence of a 3-furyl moiety. The δ 7.56 proton is also coupled (J = 0.8 Hz) to a proton at δ 5.94. The latter is directly bonded to a carbon (δ 80) that probably carries an oxygen function. Two CO_2CH_3 groups are also apparent in the ^1H and ^{13}C spectra, while the δ 208 signal in the ^{13}C spectrum indicates a ketonic carbonyl. It is probable that the remaining oxygen is in a lactone (with ^{13}C in the δ 164–177 range). The only other signals in the ^1H spectrum are multiplets associated with hydrogens at saturated centers, and, from the observed couplings, they can be assigned to one isolated CH_2CH_2 unit and one isolated CH_2CH unit.

While these data reveal the nature of some of the structural units present, they provide very little information concerning how they are interconnected. Since coupled protons occur only in small isolated groups (the longest sequence of protonated carbons is two carbons long), a correlation experiment such as ^1H-COSY[6] would provide no further useful information.[7] However, an indirect ^{13}C–^1H shift-correlated spectrum,[8] i.e., with delay times optimized for polarization transfer via $^2J_{CH}$ and/or $^3J_{CH}$, is ideally suited for investigation of such a molecule. Among the many *H*–C–*C*, *H*–C–C–*C*, and *H*–C–X–*C* (where X ≡ heteroatom) connectivities which can be established from such a spectrum are two-bond and three-bond connectivities between different protons and a specific nonprotonated carbon as well as three-bond connectivities from one proton to a different protonated carbon through either a nonprotonated carbon or a heteroatom such as oxygen. These allow one not only to assign nonprotonated carbons which link specific sequences of protonated carbons but also to tie together different segments of the molecule, thus assigning the structure.[9]

Table I. Assigned ^{13}C and ^1H Chemical Shifts for Single-, Double-, and Triple-Bond ^{13}C–^1H Connectivities Used in Assigning Structures

carbon[a]	n_H[b]	δ_C[c]	δ_H (m, J)[d]	^1H–^{13}C connectivities[e]
1	0	176.95		0.98, 1.43, 3.26,[f] 3.60
2	0	46.30		0.98, 1.43, 2.19,[h] 2.55, 3.26
3	1	40.91	3.26 (d, 10)	0.98, 1.27, 1.43, 2.19,[g] 2.55 (d)[g]
4	2	34.33	2.19 (d, 17), 2.55 (dd, 10, 17)	3.26 (d)[f]
5	0	173.67		2.19, 2.55, 3.26,[f] 3.68
6	0	61.45		1.27, 2.16, 2.19,[g] 2.29,[g] 3.26,[f] 5.87
7	0	208.41		1.27, 2.04,[f,i,j] 3.26,[f,i] 5.87
8	1	128.89	5.87 (q, 1.3)	2.04
9	0	175.25		2.04, 2.29,[f,i] 5.87[f]
10	0	68.95		1.27, 1.56,[h] 2.04, 2.16[g,i]
11	2	28.31	2.16 (dd, 15, 6), 2.29 (ddd, 15, 13, 6)	1.27,[f,i,j] 1.56 (m), 1.71 (m)
12	2	34.39	1.56 (dd, 13, 6), 1.71 (td, 13, 6)	1.16, 2.16 (m),[g,i] 2.29 (m)[g,i]
13	0	46.57		1.16, 1.56, 2.16, 5.90, 5.94[f,i]
14	0	173.24		1.16, 1.56, 2.16, 5.90,[f] 5.94[f]
15	1	117.45	5.90 (s)	
16	0	164.25		5.90,[f] 5.94[f,i]
17	1	79.95	5.94 (d, 0.8)	1.16, 1.71[g]
18	0	120.85		5.94,[h] 7.44, 7.56[h]
19	1	108.51	6.38 (dd, 1.7, 0.8)	5.94, 7.44,[f] 7.56[h]
20	1	142.86	7.44 (t, 1.7)	6.38,[f] 7.56[f]
21	1	140.25	7.56 (dt, 1.7, 0.8)	5.94,[f] 6.38,[f] 7.44[f]
22	3	18.99	1.16 (s)	1.55,[g] 1.71,[g] 5.94
23	3	16.37	2.04 (d, 1.3)	5.87
24	3	23.65	1.27 (s)	3.26[f]
25	3	27.80	0.98 (s)	1.43, 3.26[f,i]
26	3	20.67	1.43 (s)	0.98, 3.26[f]
27	3	51.25	3.68 (s)	
28	3	51.98	3.60 (s)	

[a] Carbon number is shown below. The numbering is arbitrary and is without biogenetic implications. [b] Number of attached hydrogens. [c] ^{13}C chemical shift relative to internal $(CH_3)_4Si$. [d] ^1H chemical shift(s) of attached proton(s) relative to internal $(CH_3)_4Si$. The values in parentheses indicate multiplicities (s = singlet, d = doublet, t = triplet, q = quartet) followed by observed coupling constants (in Hz). [e] ^1H–^{13}C cross-peaks observed in XCORFE spectra. The symbols in parentheses indicate multiplicities in cases where a peak is split by vicinal ^1H–^1H coupling (d = doublet, m = multiplet). [f] Peaks which are significantly more intense for T = 0.128 s (see text). [g] Peaks which are significantly more intense for T = 0.092 s. [h] Peaks which are significantly more intense for T = 0.063 s. [i] Very weak cross-peaks. [j] Apparent four-bond connectivity to methyl proton ^1H signal.

(2) Reynolds, W. F.; Hughes, D. W.; Perpick-Dumont, M.; Enriquez, R. G. *J. Magn. Reson.* **1985**, *63*, 413.

(3) A preliminary account of the determination of the structure of guyanin has been given in the following: Jacobs, H.; Ramdayal, F.; Reynolds, W. F.; McLean, S. *Tetrahedron Lett.* **1986**, *27*, 1453. The absolute stereochemistry illustrated in **1** is arbitrary since only relative stereochemistry has been determined.

(4) Doddrell, D. M.; Pegg, D. T.; Bendall, M. R. *J. Magn. Reson.* **1982**, *48*, 323.

(5) (a) Bax, A.; Morris, G. A. *J. Magn. Reson.* **1981**, *42*, 501. (b) Bax, A. *J. Magn. Reson.* **1983**, *53*, 517.

(6) Bax, A.; Freeman, R. *J. Magn. Reson.* **1981**, *44*, 542.

(7) In principle, a COSY sequence with additional delay times optimized for long-range ^1H–^1H coupling constants[6] might provide connections between different sequences of protonated carbons. However, this would provide no information about nonprotonated carbons.

(8) Hallenga, K.; van Binst, G. *Bull. Magn. Reson.* **1980**, *2*, 343.

(9) Reynolds, W. F.; Enriquez, R. G.; Escobar, L. I.; Lozoya, X. *Can. J. Chem.* **1984**, *62*, 2421.

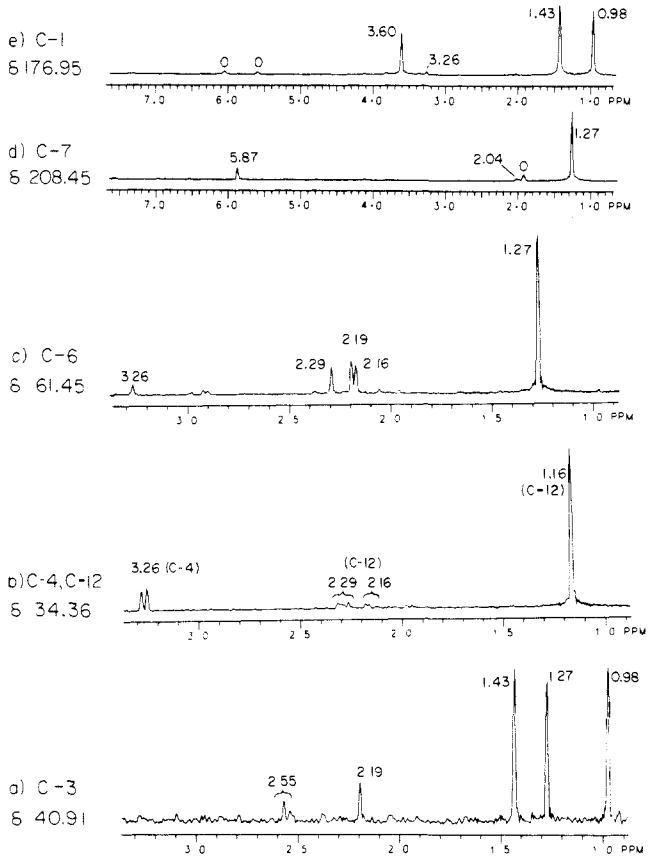

Figure 1. Typical ^1H cross sectional XCORFE spectra through specific carbon frequencies, (a) C-3, obtained with $T = 0.092$ s. (b) Cross section shows peaks associated with two overlapping ^{13}C signals (C-4, δ 34.33 and C-12, δ 34.39), obtained with $T = 0.092$ s. Peaks were assigned to individual carbons by taking cross sections through each shoulder of unresolved peak. Full ^1H spectrum shows a further peak at δ 5.94 associated with C-12. (c) C-6, obtained with $\delta = 0.092$ s. Full ^1H spectrum shows an additional peak at δ 5.87. Note that peaks at δ 2.19, δ 2.29 were not observed in a spectrum with $T = 0.063$ s[3]. (d) C-7, obtained with $T = 0.063$ s. Peak marked by circle is an artifact not totally suppressed by use of ^{13}C composite pulses. Weak peak at δ 2.04 is an apparent four-bond connectivity from H-23. It is significantly more intense in a spectrum with $T = 0.128$ s. (e) C-1, obtained with $T = 0.063$ s. Peak at δ 3.26 is significantly more intense in a spectrum with $T = 0.092$ s.

The ability to establish connectivities through heteroatoms is a particularly important feature for structural elucidation.[10] Guyanin, **1**, with 11 nonprotonated carbons and eight heteroatoms among its 36 heavy atoms, is ideal to illustrate the power of the indirect connectivity experiment,

(b) Deduction of the Complete Skeletal Structure 1 from Indirect ^{13}C–^1H Shift-Correlated Spectra. These spectra were obtained using a modified version[11,12] of our XCORFE sequence.[2] The specific modifications are described in the Experimental Section, while a more complete discussion of their effectiveness is given elsewhere.[12] They are designed to suppress two types of artifacts. The first are cross-peaks corresponding to directly bonded ^{13}C–^1H pairs. These are easily recognized since they occur at predictable frequencies.[2] Nevertheless, it is helpful to suppress them since they obscure real long-range connectivities. The second, more serious, artifacts are those arising from pulse imperfections, etc. since these occur at unpredictable frequencies[12] and could be mistaken for real correlations. Guyanin **1** is a particularly difficult challenge in this regard since the wide range of ^{13}C–^1H one-bond couplings and ^{13}C and ^1H chemical shifts promote the formation of artifacts. Nevertheless, as can be seen from the cross-sectional spectra in Figure 1, the incorporated modifications have suppressed artifact peaks to the point where they are lower in intensity than all but the weakest of the real peaks. This, combined with the fact that the artifact peaks are almost always broader than the real peaks[12] and usually occur at f_1 (^1H) frequencies at which there is no actual ^1H peak, makes it easy to distinguish real and artifact peaks. Finally, each part structure and each connectivity between part structures was established from several ^{13}C–^1H cross-peaks. This great redundancy of information makes this approach to structure elucidation particularly reliable.

The initial XCORFE spectrum was obtained by using a fixed delay, T, prior to polarization transfer of 0.063s[3]. This corresponds to optimum polarization transfer for $^nJ_{CH} = 8$ Hz ($T = 1/2J_{CH}$). With this delay, more than a sufficient number of cross-peaks were observed to allow unambiguous structural assignment.[3] However, not all possible peaks were observed. One likely reason for this is that many of the $^nJ_{CH}$ couplings should be significantly smaller than 8 Hz,[13] resulting in inefficient polarization transfer. In addition, one problem with XCORFE[2] and related sequences[14,15] which have a constant delay prior to polarization transfer is that signal intensity is lost if ^1H–^1H coupling vectors are antiphase at the end of T.[14] This occurs for $T = 1/2J_{HH}$, $3/2J_{HH}$, etc., while polarization transfer is maximum for $T = 1/J_{HH}$, $2/J_{HH}$, etc. Because of the range of J_{HH} values for **1** (see Table I), it is impossible to choose a single value of T which avoids the former condition for all protons. In view of the unusual nature of the proposed structure and the fact that we were evaluating a new pulse sequence, it was considered desirable to observe as many of the potential cross-peaks for **1** as possible. Consequently, additional spectra were obtained by using $T = 0.092$ s and $T = 0.128$ s, respectively, optimized for J_{CH} values of ca. 5.5 and 4 Hz. In the latter case, it was necessary to divide the ^{13}C spectral window in half and record two separate spectra, due to disk storage limitations. Almost all of the previously unobserved connectivities were observed in one or more of these spectra while others observed for $T = 0.063$ s were missing or reduced in intensity. All observed ^1H–^{13}C connectivities are summarized in Table I with typical ^1H cross sectional spectra through specific ^{13}C frequencies illustrated in Figure 1.

The starting point for structural assignment was the observation that, for a pair of methyl groups (at δ_C 27.8, δ_H 0.98 and δ_C 20.7, δ_H 1.43), cross-peaks were observed for each methyl carbon with the other methyl protons. This requires the presence of a *gem*-dimethyl group.[16] The *gem*-dimethyl protons also showed cross-peaks with the δ 40.9 methine carbon and nonprotonated carbons at δ 46.3 and δ 177.0. The latter carbon also showed a cross-peak with one of the methoxyl ^1H signals, indicating that it is an ester carbon, while the methine proton (δ 3.26) shows weak cross-peaks with the two *gem*-dimethyl carbons. These data are consistent only with the part structure **2**.

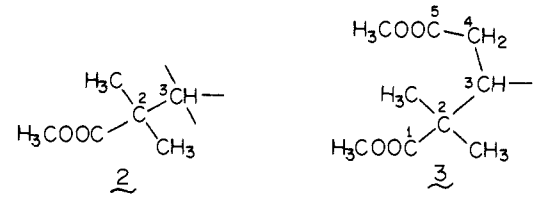

C-3 also shows cross-peaks with the methylene protons at δ 2.19 and δ 2.55. The latter appears as a doublet due to coupling to the methine proton, confirming a two-bond connectivity.[17] Similarly, the methylene carbon (δ 34.3) shows a doublet peak

(10) Taylor, D. A. H. *Tetrahedron* **1987**, *43*, 2779.
(11) Perpick-Dumont, M., M.Sc. Thesis, University of Toronto, 1986.
(12) Perpick-Dumont, M.; Enriquez, R. G.; McLean, S.; Reynolds, W. F. *J. Magn. Reson.* **1987**, *75*, 414.
(13) Hansen, P. E. *Prog. Nucl. Magn. Reson. Spectrosc.* **1981**, *14*, 175.
(14) Bauer, C.; Freeman, R.; Wimperis, S. *J. Magn. Reson.* **1984**, *58*, 526.
(15) Kessler, H.; Griesenger, C.; Zarbock, J.; Loosli, H. R. *J. Magn. Reson.* **1984**, *57*, 331.
(16) Reynolds, W. F.; McLean, S.; Poplawski, J.; Enriquez, R. G.; Escobar, L. I.; Leon, I. *Tetrahedron* **1986**, *42*, 3419.
(17) See Figure 1a. The XCORFE sequence distinguishes two-bond from three-bond H–C connectivities involving protonated carbons, since the former are split by vicinal ^1H–^1H coupling, while the latter appear as singlets. The absence of any splitting for the δ 2.19 proton reflects the near zero coupling of this proton to H-3; see Table I.

due to the methine proton, while all three protons also show cross-peaks with a nonprotonated carbon at δ 173.7. Since the latter carbon also has a cross-peak with a second OCH_3 ^1H signal, it must be part of the second ester group. This group could be bonded to either C-3 or to the CH_2 group. However, C-3 shows a further cross-peak with a methyl ^1H singlet (δ 1.27), indicating bonding to some other part of the molecule. These data indicate partial structure **3**. While there appears to be no precedent for this type of structure in terpene chemistry, we regard it as unambiguously established since every possible two-bond and three-bond C–H connectivity within this structural fragment was observed.

Both H-3 and one of the H-4 protons (δ 2.55) also show cross-peaks with a nonprotonated carbon at δ 61.5 which must represent the point of attachment of **3** to the rest of the molecule. This carbon, along with nonprotonated carbons at δ 69,0 and δ 208.4 (assigned previously as a carbonyl) all show cross-peaks with the above-mentioned methyl ^1H singlet. The δ 69.0 carbon also shows a cross-peak with the methyl ^1H peak at δ 2.04, which shows further cross-peaks with the nonprotonated carbon at δ 175,3 and the methine carbon at δ 128.9. Finally the methine proton at δ 5.87 (which is bonded to the above-mentioned δ 128.9 carbon) shows cross-peaks with the δ 208.4, δ 175.3, δ 69.0 and δ 61.5 carbons, along with the methyl carbon at δ 16.4 (which is bonded to the methyl protons at δ 2.04). The only structure consistent with the patterns of connectivities outlined above is **4**. C-10 also

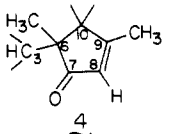

4

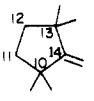

5

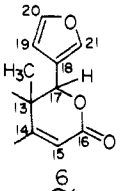

6

shows cross-peaks with the methylene protons at δ 2.16, δ 2.29 (both of which are bonded to the carbon at δ 28.3) plus the methylene proton at δ 1.56 (bonded to the carbon at δ 34.4). The former two protons also show cross-peaks with C-6 and C-9. This indicates a CH_2CH_2 linkage bonded to C-10 with the δ 28.3 carbon forming the point of attachment. Both sets of methylene protons also show cross-peaks with nonprotonated carbons at δ 46.6 and δ 173.2. The fact that all methylene protons show cross-peaks with the same three nonprotonated carbons, including C-10, is consistent only with a second five-carbon ring incorporating C-10 (see **5**). It follows that C-10 is a spiro center linking **4** and **5**.

Similar information concerning two- and three-bond connectivities was used to deduce the remaining structural fragments, i.e., an α,β-unsaturated lactone **6** and the anticipated furan ring which is bonded to C-17. Putting the separate fragments together gave the final skeletal structure of guyanin as shown in **1**. Note that each fragment as well as the connections between different fragments have been determined with considerable redundancy due to the vast amount of connectivity information obtained from the XCORFE spectra.

(c) X-ray Crystal Structure Analysis of 1 and Comparison of Solution and Solid-State Structures. The connectivities observed in the initial XCORFE experiment (with T = 0.063 s) allowed the structure of guyanin to be assigned with a high degree of confidence.[3] However, since this was the first application of this method to the assignment of structure to a previously unknown compound of some complexity, it was deemed advisable to confirm the assignment and define the stereochemistry (relative configuration) of the molecule by X-ray crystal structure analysis. Fortunately, guyanin was readily obtained as crystals suitable for this purpose, and the X-ray analysis was carried out while the further XCORFE experiments described above were in progress. Figure 2 shows the structure determined by the X-ray method, and the heavy atom coordinates are listed in Table II. As can be seen, the original assignment of structure is confirmed, and the stereochemistry is now defined.

Comparison of hydrogen atom coordinates from the crystal structure with certain NMR parameters in solution indicates that

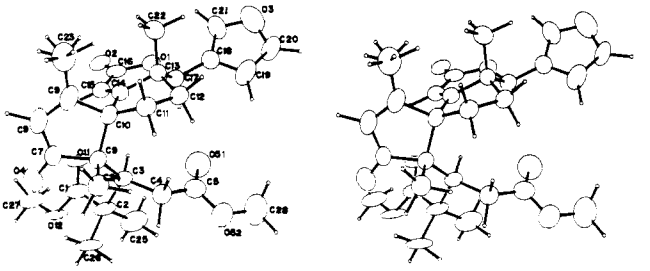

Figure 2. ORTEP stereoprojection for **1**. Absolute stereochemistry is arbitrary.

Table II. Final Atomic Positional (×10⁴) and Thermal (×10³) Parameters

atom	x	y	z	U_{eq}[a] (Å²)
O(1)	6061 (2)	−749 (2)	2050 (1)	52 (1)
O(2)	7927 (3)	−187 (3)	1670 (1)	85 (2)
O(3)	2293 (3)	−1671 (3)	1724 (2)	100 (3)
O(4)	10587 (3)	−936 (2)	4273 (1)	81 (2)
O(11)	9113 (3)	705 (2)	3452 (1)	72 (2)
O(12)	10198 (3)	1516 (2)	4275 (1)	86 (2)
O(51)	4911 (3)	168 (2)	4030 (1)	76 (2)
O(52)	4425 (3)	54 (2)	5111 (1)	64 (2)
C(1)	9263 (4)	872 (3)	4040 (2)	64 (2)
C(2)	8355 (4)	490 (3)	4582 (2)	56 (2)
C(3)	7585 (3)	−540 (2)	4344 (1)	44 (2)
C(4)	6382 (3)	−709 (3)	4790 (2)	47 (2)
C(5)	5193 (4)	−98 (3)	4582 (2)	51 (2)
C(6)	8349 (3)	−1639 (3)	4269 (1)	43 (2)
C(7)	9810 (4)	−1614 (4)	4076 (2)	57 (2)
C(8)	10101 (4)	−2561 (4)	3701 (2)	60 (2)
C(9)	9029 (4)	−3083 (3)	3517 (2)	54 (2)
C(10)	7819 (3)	−2449 (3)	3706 (2)	41 (2)
C(11)	6620 (3)	−3156 (3)	3897 (2)	45 (2)
C(12)	5465 (3)	−2626 (3)	3556 (2)	45 (2)
C(13)	5997 (3)	−2218 (2)	2879 (1)	37 (2)
C(14)	7352 (3)	−1886 (2)	3056 (1)	39 (2)
C(15)	7989 (4)	−1169 (3)	2679 (1)	45 (2)
C(16)	7363 (4)	−659 (3)	2104 (2)	53 (2)
C(17)	5339 (3)	−1171 (3)	2621 (2)	43 (2)
C(18)	4004 (4)	−1339 (3)	2380 (2)	47 (2)
C(19)	2884 (4)	−1400 (4)	2773 (2)	87 (3)
C(20)	1864 (4)	−1591 (4)	2395 (2)	86 (3)
C(21)	3576 (4)	−1491 (4)	1738 (2)	72 (3)
C(22)	5964 (4)	−3121 (3)	2353 (2)	51 (2)
C(23)	9002 (4)	−4148 (3)	3141 (2)	71 (3)
C(24)	8416 (4)	−2272 (3)	4956 (2)	55 (2)
C(25)	7377 (5)	1451 (3)	4628 (2)	84 (3)
C(26)	9022 (4)	383 (4)	5273 (2)	82 (3)
C(27)	11038 (5)	1973 (4)	3774 (2)	106 (4)
C(28)	3170 (4)	525 (4)	4963 (2)	89 (3)

[a] $U_{eq} = (1/3)(U_{11} + U_{22} + U_{33})$.

the molecular conformation of **1** is essentially identical in solution and in the solid state. For example, there is no observable coupling between H-3 and H-4a or between H-11a and H-12a, indicating dihedral angles of near 90° between each pair of vicinal protons. The actual dihedral angles determined from the crystal structure data are 93° between H-3 and H-4a and 85° between H-11a and H-12a. Further conformational information in solution was deduced from measurements of homonuclear (^1H) nuclear Overhauser enhancement factors which were carried out to assign the *gem*-dimethyl signals. Irradiation of the methyl ^1H signal at δ 0.98 produce a significant NOE (+11%) for H-3, while no enhancement of H-3 was observed when the methyl signal at δ 1.43 was irradiated. Thus the former methyl group is assigned as C-25 and the latter as C-26 due to the much closer proximity of the C-25 protons to H-3 (see Figure 2). Both the vicinal coupling data and the NOE data suggest that there is little conformational mobility in the side chain since any conformational averaging about C2/C3 and C3/C4 bonds should, respectively, be reflected in a nonzero NOE between H-26 and H-3 and a nonzero coupling between H-3 and H-4a. Similarly the five-membered ring involving C-11 and C-12 must exist in a single conformation since

Table III. T_1 Relaxation Times (s) for the Various Protonated Carbons of **1**

carbon	T_1[a]	nT_1[b]	carbon	T_1	nT_1
3	0.49	0.49	21	0.61	0.61
4	0.26	0.52	22	0.68	2.04
8	0.44	0.44	23	1.37	4.11
11	0.26	0.52	24	0.88	2.64
12	0.26	0.52	25	0.21	0.63
15	0.42	0.42	26	0.42	1.26
17	0.52	0.52	27	1.17	3.51
19	0.61	0.61	28	1.10	3.30
20	0.52	0.52			

[a] Estimated errors in T_1 measurements (based on reproducibility from different runs) is ±3%. [b] T_1 multiplied by number of directly bonded protons.

Table IV. C–C–C Bond Angles and C–C Bond Lengths Involving C(2) and C(3), Illustrating Severe Steric Distortion in Part Structure **3**

carbons[a]	C–C–C[b] (deg)	n_{C-C}[c] (Å)
C(3)–C(2)–C(1)	110.7 (3)	
C(3)–C(2)–C(25)	107.3 (3)[d]	
C(3)–C(2)–C(26)	115.4 (3)	
C(1)–C(2)–C(25)	102.3 (3)[d]	
C(1)–C(2)–C(26)	112.5 (3)	
C(25)–C(2)–C(26)	107.6 (3)[d]	
C(2)–C(3)–C(4)	110.3 (2)	
C(2)–C(3)–C(6)	117.7 (3)	
C(4)–C(3)–C(6)	110.3 (2)	
C(2)–C(3)		1.567 (5)
C(2)–C(25)		1.558 (6)
C(2)–C(26)		1.542 (5)
C(3)–C(4)		1.544 (4)
C(3)–C(6)		1.570 (4)

[a] Numbering as shown in Table I. [b] The number in parentheses indicates the uncertainty in the final number. [c] C–C bond length. [d] Note that all three angles involving C(25) are decreased below the nominal tetrahedral angle, consistent with severe steric hindrance of rotation of this methyl group (see text).

any conformational mobility should result in a nonzero coupling between H-11 and H-12a.

Further evidence for the lack of conformational mobility in **1** is provided by T_1 relaxation times for protonated carbons (see Table III). The fact that nT_1 values for C-3 and C-4 are identical with those for the ring carbons C-11 and C-12 indicates negligible segmental motion in the side chain.[18] In fact, allowing for slightly shorter C–H bonds and consequently slightly shorter T_1 values for olefinic carbons, the nT_1 data suggest that the molecule tumbles in an essentially isotropic manner ($\tau_C \simeq 9 \times 10^{-11}$ s[18]) with some rotation of the furan ring and varying degrees of methyl rotation.

The rigidity of the side chain and the similar conformation in solution and solid states most likely reflect strong steric hindrance to bond rotation. For example, several of the C–C–C angles within the side chain vary significantly from the tetrahedral angle (see Table IV, noting particularly the 118° angle between C-2, C-3, and C-6), and a number of C–C bonds are unusually long. Further evidence for varying degrees of steric hindrance in different parts of the molecule is provided by the wide range of methyl ^{13}C T_1 values, from 0.21 s for C-25 to 1.37 s for C-23. The former value is only slightly greater than expected for a nonrotating group ($\simeq$ 0,17 s based on an average nT_1 value of 0.51 s for methylene and methine carbons), while the latter is at the upper limit expected for a freely rotating methyl group.[18] The latter observation is consistent with the crystal structure which shows two populated conformations for C-23 (see Figure 2). The hindered rotation of C-25 and, to a lesser extent, C-26 presumably reflects the steric distortions about C-2 which have decreased the C-1/C-2/C-25, C-3/C-2/C-25, and C-25/C-2/C-26 angles (see Table IV), restricting the rotational freedom of C-25 in particular.

(18) Allerhand, A.; Doddrell, D.; Komoroski, R. *J. Chem. Phys.* **1971**, *55*, 189.

Thus the overall picture which emerges is of a complex molecule with surprisingly limited conformational mobility.

(d) Biogenesis of Guyanin. With the structure of guyanin established, the question of its biogenetic origin immediately follows. It is clearly a member of the fascinating array of metabolic products resulting from biological oxidations of a tetracyclic triterpene, sometimes leading to degradation of the carbon skeleton, that are a characteristic of the botanical order Rutales *s.s.*[19] The formation of the furan and lactone moieties of guyanin by oxidation of the side chain and ring D of a precursor such as tirucallol have ample precedent,[19] but the oxidative transformation of every other ring is unusual. It is reasonable to suggest that oxidations provide an intermediate corresponding to **7**, which, by

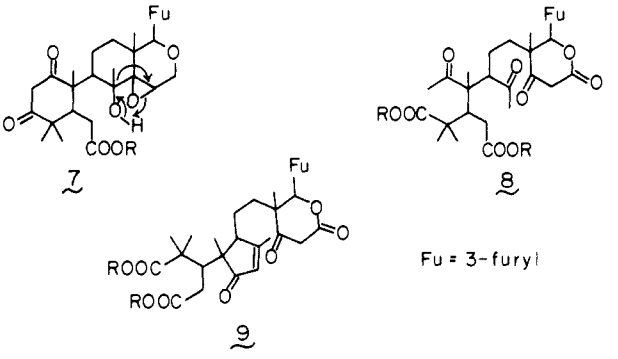

a retro-Claisen process that opens ring A and a rearrangement of the glycidol unit as shown, leads to **8**. This in turn can form the cyclopentenone **9** by an aldol condensation, and a final aldol-type cyclization with dehydration converts **9** to guyanin. Precedents for the oxidations required to form the proposed intermediate **7** are found in known tetranorterpenoids, notably methyl angolensate,[20] but it is of phytochemical interest that these precedents are found not in the Rutaceae but in the botanically related Meliaceae.

Conclusions

The structure and stereochemistry of guyanin, a novel tetranortriterpenoid, have been unequivocally assigned. While these assignments are of some significance in their own right, the most important conclusion from the present investigation is that the 2D NMR method, with heteronuclear shift correlation data obtained with the XCORFE sequence to establish units of molecular connectivity, can be used to unambiguously elucidate the structure of a complex organic molecule of unprecedented structure. Its application differs in important aspects from that of the earlier methods of one-dimensional NMR which depend on the empirical assignment of chemical shifts. As has been shown previously, the latter approach can lead to incorrect structural assignments.[21]

The status of X-ray crystallography as the definitive method for determining organic structure and especially stereochemistry, provided that a suitable crystal is available, cannot be challenged. However, 2D NMR provides a powerful investigative tool which complements the X-ray method in many respects. The solubility of the sample, rather than its crystallinity, is the critical physical property. One-bond and long-range ^{13}C–^1H shift-correlated spectra provide structural information in a semiroutine manner[22] and can be readily incorporated into protocols for investigating structures of natural products, along with other 2D spectra such

(19) Waterman, P. G.; Grundon, M. F. *Chemistry and Chemical Taxonomy of the Rutales*; Academic Press: London, 1983.

(20) (a) Bevan, C. W. L.; Powell, J. W.; Taylor, D. A. H.; Halsall, T. G.; Toft, P.; Welford, M. *J. Chem. Soc. C* **1967**, 163. (b) Chan, W. R.; Magnus, K. E.; Mootoo, B. S. *J. Chem. Soc. C* **1967**, 171.

(21) McLean, S.; Perpick-Dumont, M.; Reynolds, W. F.; Jacobs, H.; Lachmansing, S. S. *Can. J. Chem.* **1987**, *65*, 2519.

(22) For a review of earlier utilization of long-range ^{13}C–^1H shift-correlation spectra for partial structural assignment and spectral assignment, see: Martin, G. E. *Magn. Reson. Chem.* **1988**, in press. The present investigation goes beyond earlier investigations in the extent on which it relies on these data for structural assignment and the uniqueness of the structure which has been assigned.

Table V. Crystal Data, Details of Intensity Measurements and Structure Refinements[a]

compound	guyanin
formula	$C_{28}H_{34}O_8$
system	orthorhombic
$a \times b \times c$ (Å)	10.364 (6) × 12.269 (3) × 19.848 (4)
U (Å^3)	2524
fw/Z/d_{calcd} (g cm^{-3})	498.6/4/1.312
space group	$P2_12_12_1$
μ(Mo K$\bar{\alpha}$) (cm^{-1})	0.9
reflcns in cell detmn	25/(8.3 < θ < 12.6°)
scan widths (deg)	0.95 + 0.35 tan θ
max. scan time (s)	90
std reflcns (interval s)	3/9500[b]
max. 2θ (deg)/octants	55/h,k,±l[c]
total data collctd	6207 (inc. stds)
unique data	4956[d]
structure soln	direct methods (small fragment), several cycles least-squares/Fourier calculations
H atoms	located in ΔF maps and geometries then optimized[e]
no. of obsd data	3039 [$I \geq 3\sigma(I)$]
final R (wR)	0.0496 (0.0491)
max. Δ/σ final cycle	0.14 (2 blocks)
weights, value of p[f]	0.00033
max. peak final ΔF map	0.25 eÅ^{-3}
programs	Enraf-Nonius SDP package on PDP11/23 and SHELX on Gould 9705 computers
scattering factors	from *International Tables for X-ray Crystallography*

[a] Enraf-Nonius CAD4 diffractometer; Mo K$\bar{\alpha}$ radiation (graphite monochromator); λ = 0.71069 Å; T = 298 K; ω-2θ mode; Lorentz and polarization corrections applied to all data collected. [b] No significant losses in intensities observed. [c] h,k,l for $h \geq 10$. [d] 180 standard reflections and a further 676 reflections which were systematically absent or had F_{obsd} = 0.0 rejected. 395 symmetry equivalent data then averaged ($R_{merg}(F)$ = 0.02) to give indicated number of unique data. [e] Two locations found for methyl group C(23)H$_3$. [f] Weights given by $[\sigma^2(F) + pF^2]^{-1}$.

as COSY spectra[6] and NOE spectra.[23]

Experimental Section

Isolation of **1** is described in detail elsewhere.[24] All NMR spectra were recorded on a Varian XL-400 spectrometer by using 5 mm multinuclear and ^{1}H probes (multinuclear probe ^{13}C 90° pulse width = 13.9 μs, ^{1}H 90° pulse width (through decoupler coils) = 26 μs). The XCORFE pulse sequence was modified by replacing the initial ^{1}H 90° pulse by a TANGO pulse sandwich,[25] which acts as a 90° pulse only for protons not directly bonded to ^{13}C, and by replacing ^{13}C 180° pulses by composite 180° pulses.[26] The former gave more effective suppression of cross-peaks due to directly bonded ^{13}C–^{1}H pairs, while the latter minimized artifacts which arose from incomplete inversion by the finite ^{13}C 180° pulses near either end of the ^{13}C spectral window.[12,26] More complete details are given elsewhere.[12] The sample consisted of 90 mg of **1** dissolved in ca. 0.5 mL of $CDCl_3$. A typical set of acquisition parameters for XCORFE spectra involved collecting 4096 data points for an f_2 (^{13}C) spectral width of 20 000 Hz, an f_1 (^{1}H) spectral width of 2800 Hz with 352 time increments (zero filled to 1024), 160 transients per time increment, a relaxation delay of 0.8 s, a fixed delay prior to polarization transfer of 0.063 s, and a refocussing delay of 0.032 s after polarization transfer. ^{13}C T_1 measurements were carried out by using a standard inversion-recovery sequence incorporating ^{13}C composite 180° pulses.[26] T_1 values were determined by exponential fitting, with standard Varian software.

Crystals of **1**, mp 261–262 °C, suitable for X-ray analysis were obtained by recrystallization from methanol. Further work on the diffractometer gave the crystal data summarized in Table V, which also contains details of the intensity measurements and structure refinements undertaken. Least-squares refinements in two large blocks and minimizing $\Sigma\omega\Delta F^2$ then converged (H-atoms in calculated positions, all non-hydrogen atoms with anisotropic thermal parameters) to the indicated residuals. There was no significant difference observable on refinement of the alternative "hand". Final atomic positional and equivalent isotropic thermal parameters for the non-hydrogen atoms are given in Table II.

Acknowledgment. The Centre at the University of Guyana was supported by the Canadian International Development Agency, and the research at the University of Toronto was supported by grants from the Natural Sciences and Engineering Research Council of Canada.

Supplementary Material Available: Tables of hydrogen atom parameters, anisotropic thermal parameters, bond lengths and bond angles, and torsion angles (10 pages); listing of observed and calculated structure factors (13 pages). Ordering information is given on any current masthead page.

(23) For example, see: Saunders, J. K. M.; Hunter, B. K. *Modern NMR. A Guide for Chemists*; Oxford University Press: Oxford, 1987. NOE spectra can often give useful stereochemical information.

(24) Jacobs, H.; Ramdayal, F.; McLean, S.; Perpick-Dumont, M.; Puzzuoli, F.; Reynolds, W. F. *J. Nat. Prod.* **1987**, *50*, 507.

(25) Wimperis, S.; Freeman, R. *J. Magn. Reson.* **1984**, *58*, 348.

(26) Levitt, M.; Freeman, R. *J. Magn. Reson.* **1979**, *33*, 473.